

Magnetic field impact on the high and low Reynolds number flows

L. Pleskacz and E. Fornalik-Wajs

Department of Fundamental Research in Energy Engineering, AGH Univeristy of Science and Technology, 30 Mickiewicz Ave, 30-059 Krakow, Poland

E-mail: pleskacz@agh.edu.pl

Abstract. The effect of a strong magnetic field on the temperature and velocity fields of laminar flow was examined. The magnetizing force and gravity term were included in the momentum conservation equation. Biot-Savart's law was applied to obtain the distribution of magnetic field. Three-dimensional computations were performed for straight pipe and pipe with elbow. The single circular magnetic coil was oriented perpendicularly to the flow axis and divided the straight pipe in two equal parts, while in the case of pipe with elbow was just at the beginning of elbow.. The wall of the first straight part was adiabatic while the second was isothermal. Half of the elbow was heated, while the remaining part was adiabatic. Various boundary conditions were applied to estimate their influence on the velocity and temperature distributions. Low entrance velocity, high wall temperature and strong magnetic field led to deceleration of the flow in the central area, acceleration near the wall and formation of recirculation zone in between for the straight pipe. Flow structure and temperature field in the pipe with elbow were significantly modified by the magnetic force. Increasing entrance velocity reduced influence of magnetic field, therefore the flow was less modified. High temperature and magnetic induction resulted in significant changes of the velocity profile. The analysis was conducted with an application of software with special user-defined function. The magnetic field had an influence on the forced convection but its scale depended on the fluid and flow properties, boundary conditions and magnetic field induction.

1. Introduction

All elements and ordinary substances show some magnetic effects, although very small ones – a thousand to a million times less than the effects in ferromagnetic materials [1]. It has come out that this small magnetism can be also utilized. Due to a development of superconducting magnets, the strong magnetic field could be generated and the new interesting phenomena could be discovered, for example: magnetic levitation of weakly magnetic substances, magnetic breath support, magnetothermal wind, Wakayama jet, etc. [2] [3] [4] [5] [6] [7]. Magnetothermal wind [6] was one of these new phenomena. It concerned appearance of wind in a partially heated tube placed in the strong magnetic field. The warm air was expelled from the magnet while the cold air was sucked into it.

The concept of introduction of convection showed new possibility of magnetic field utilization – heat transfer enhancement, which is very important nowadays. Transfer of high heat fluxes and better energy utilization are ones of the main engineering concerns. Therefore magnetothermal convection in the closed enclosures was extensively studied afterwards. The experimental and numerical investigations were carried out by [8] [9] [10] [11] [12] [13] [14] [15] [16] [17]. They



proved the influence of magnetic field on the natural convection of paramagnetic and diamagnetic substances and their heat transfer. The magnetic convection from the engineering point of view was presented in a book [18]. One of the chapters described the magnetothermal wind tunnel, which connected the problem reported by [6] (appearance of magnetothermal wind) with the classical Graetz problem [19], which referred to forced convection through a pipe with partially heated wall. The Graetz problem was investigated by many researchers in various fields (due to its usability) [20] [21] [22]. They analyzed also extended Graetz problem (with thermal conduction) and problems with various boundary conditions.

The case studied by Ozoe [18] was a first example (found by Authors) of the magnetic field influence on the forced convection of weakly magnetic substances. The two-dimensional flow of air was analyzed and the strong influence of magnetic field on it was found in the region close to the magnetic coil. It resulted in higher values of Nusselt number. The presented paper is a continuation of this problem. Authors undertake the matter of three-dimensional model with variable parameters like the geometry, inlet velocity, wall temperature and magnetic induction. It led to the detail description of flow in the region with significant influence of the magnetic field.

2. Mathematical model

With basic assumptions including: incompressible flow, lack of additional mass source, stationary, laminar, three-dimensional flow, the continuity equation may be represented by following equation:

$$\nabla \cdot \vec{u} = 0, \quad (1)$$

where: \vec{u} - velocity m/s.

Employing conditions presented above complemented with the gravitational and magnetic forces (5) treated as the external body forces led to the momentum equation in following form:

$$\rho (\vec{u} \cdot \nabla \vec{u}) = -\nabla p + \mu \nabla^2 \vec{u} + \vec{F}_b, \quad (2)$$

where ρ - density kg/m³, μ - dynamic viscosity Pa·s, p - pressure Pa, g - gravitational acceleration m/s², $\vec{F}_b = F_g + F_{mag}$ - body forces N/m³, F_g - gravitational force N/m³, F_{mag} - magnetic force N/m³.

The following formula describes energy equation:

$$\vec{u} \cdot \nabla T = \frac{\lambda}{\rho c_p} \nabla^2 T, \quad (3)$$

where: T - temperature K, λ - thermal conductivity W/(m·K), ρ - density kg/m³, c_p - specific heat J/(kg·K), with following assumptions: viscous dissipation and species diffusion are negligible, flow is steady, there is lack of external heat source.

In order to calculate the distribution of magnetic field around single circular coil, Biot-Savart's law was applied [23]:

$$\vec{B} = \frac{\mu_m i}{4\pi} \oint_c \frac{d\vec{s} \times \vec{r}}{|\vec{r}|^3}, \quad (4)$$

where: \vec{B} - magnetic induction vector T, μ_m - magnetic permeability H/m, i - current magnitude A, $d\vec{s}$ - infinitely small element of the coil m, r - radius of coil m, \vec{r} - position vector m.

Placing examined flows of paramagnetic fluid in magnetic field described by above equation, resulted in the flow being affected with a new kind of influence, known as the magnetic force. This force was included in the Navier-Stokes equations as another external body force [24]:

$$\vec{F}_{mag} = - \left(1 + \frac{1}{T_0 \beta} \right) \frac{\chi \rho \beta (T - T_0)}{2\mu_m} \vec{\nabla} B^2, \quad (5)$$

where: $T_0 = (T_w + T_f)/2$ - reference temperature K, T_w - wall temperature K, T_f - fluid temperature K, β - volumetric thermal expansion coefficient K^{-1} , χ - volumetric magnetic susceptibility -.

3. Studied case and applied solutions

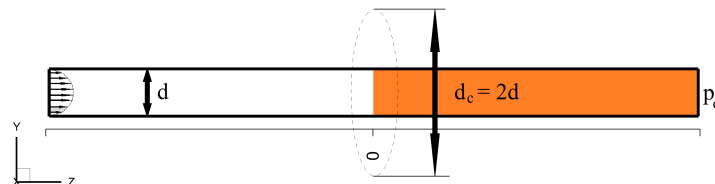


Figure 1. The schematic view of straight pipe.

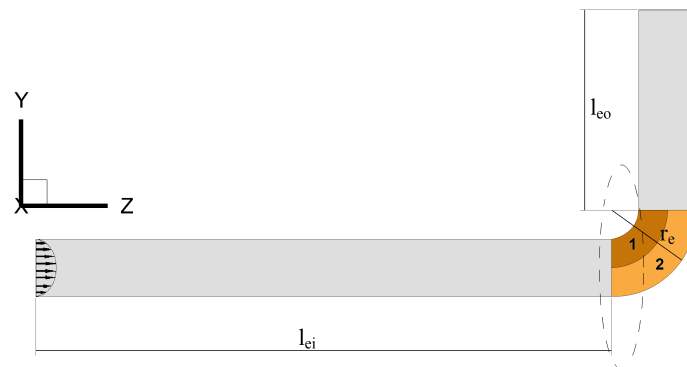


Figure 2. The schematic view of pipe with an elbow

The first studied geometries were circular straight three-dimensional ducts of diameter $d = 0,04$ m and $l = 1$ m. The straight pipe geometry is presented in figure 1. While studying the presented data, reader's attention should be given to the model's orientation in the coordinate system. The magnetic coil was set in XY plane, that was normal to Z-axis and it was origin of the system. The plane containing the magnetic coil divided the pipe in two equal parts. The wall of the first part was adiabatic while the second was isothermal.

The second studied geometry was pipe with an elbow of diameter $d_e = 0.01$ m. It consisted of an inlet section of length $l_{ei} = 0.1$ m, an elbow section with external radius $r_e = 0.015$ m and outlet section of length $l_{eo} = 0.035$ m. The magnetic coil was set just ahead of the elbow. The wall of the elbow was divided in two isothermally heated parts, from now on known as variant 1 and variant 2. This geometry is schematically presented in figure 2.

The diameter of the coil was always twice that of a pipe. The parabolic velocity profile was assumed at the inlet. Table 1 presents the thermophysical and magnetic properties of a fluid used in calculations. The inlet fluid temperature was $T_f = 300$ K in all studied cases. At the outlet pressure was assumed to be $p_o = 101325$ Pa.

The academic license software (GAMBIT 2.4 and Fluent 6.3) was used to generate the grid and perform the numerical computations. The special user-defined function calculating the distribution of magnetic force and three dimensional parabolic velocity profile were implemented in the code. The grid consisted of 147400 wedge elements for the straight pipe and 186800 wedge elements for pipe with elbow.

Table 1. Thermophysical and magnetic properties of air.

density	dynamic viscosity	volumetric thermal expansion coefficient	magnetic susceptibility	magnetic permeability	specific heat	thermal conductivity
ρ	μ	β	χ	μ_m	c_p	λ
kg/m ³	Pa·s	K ⁻¹	-	H/m	J/(kg·K)	W/(m·K)
1.225	$1.7894 \cdot 10^{-5}$	$3.33 \cdot 10^{-3}$	$3.77 \cdot 10^{-7}$	$4\pi \cdot 10^{-7}$	1006.43	$2.42 \cdot 10^{-2}$

4. Results and discussion

4.1. Analysis of inlet velocity influence on velocity and temperature distributions

In this numerical case the pipe of diameter $d = 0.04$ m and length $l = 1$ m was studied. The analysis of inlet velocity influence on the velocity and temperature distributions was conducted with constant magnitude of magnetic induction in the centre of the coil $b_0 = 8$ T and constant value of temperature of the wall $T_w = 350$ K. The varying parameter in this case was average inlet velocity U_{avg} .

Figure 3 presents the influence of average inlet velocity on the velocity distribution in the magnetic field. The degree of profile's deformation against the profile in the flow without magnetic field depended on examined parameter. Application of the lowest average inlet velocity (0.2 m/s, $Re = 547$) resulted in appearing of the greatest deformation of parabolic velocity profile (figure 3(a)).

While taking into account the highest average inlet velocity (figure 3(c)) these deformations are minimal. The profiles remained parabolic on the whole examined cross section. The results might be divided in two groups. First of them was the group of distorted velocity profiles and contained cases of average inlet velocities of 0.2 m/s and 0.5 m/s (figure 3(a) and 3(b)). The second group consisted of the one case remained, where the gentle flattening of the profile's sides near the electric coil and narrowing or tearing of the flow's central area were the only expressions of profiles' change (figure 3(c)).

In the group of distorted velocity profiles the characteristic profile with three peaks could be observed. However, it vanished in the case of $U_{avg} = 0.5$ m/s ($Re = 1369$). Behind the magnetic coil the area of flow slowing down appeared.

Acceleration near the wall was caused by the magnetic force. It was compatible with the flow direction. As the velocity increased, the magnetic force effect weakened, which was related to thermal boundary layer narrowing.

The effect of flow suppression reduced while moving closer to the flow axis due to the drop of temperature (and in consequence, value of temperature difference) and of magnetic induction magnitude (caused by drifting away from electric coil) and what's more important the magnetic force from eq. (5).

The central area of each profile preserved parabolic shape (though the maximum velocity magnitude decreased) and the greatest change took place beyond it.

No recirculation zone was observed in any of examined cases. Nonetheless, it could occur with the increase of magnetic force acting on fluid or further decrease of average inlet velocity.

4.2. Analysis of wall temperature influence on velocity and temperature distributions

The analysis of wall temperature influence on the velocity and temperature distributions in the pipe of diameter $d = 0.04$ m and length $l = 1$ m was conducted with constant magnitude of the

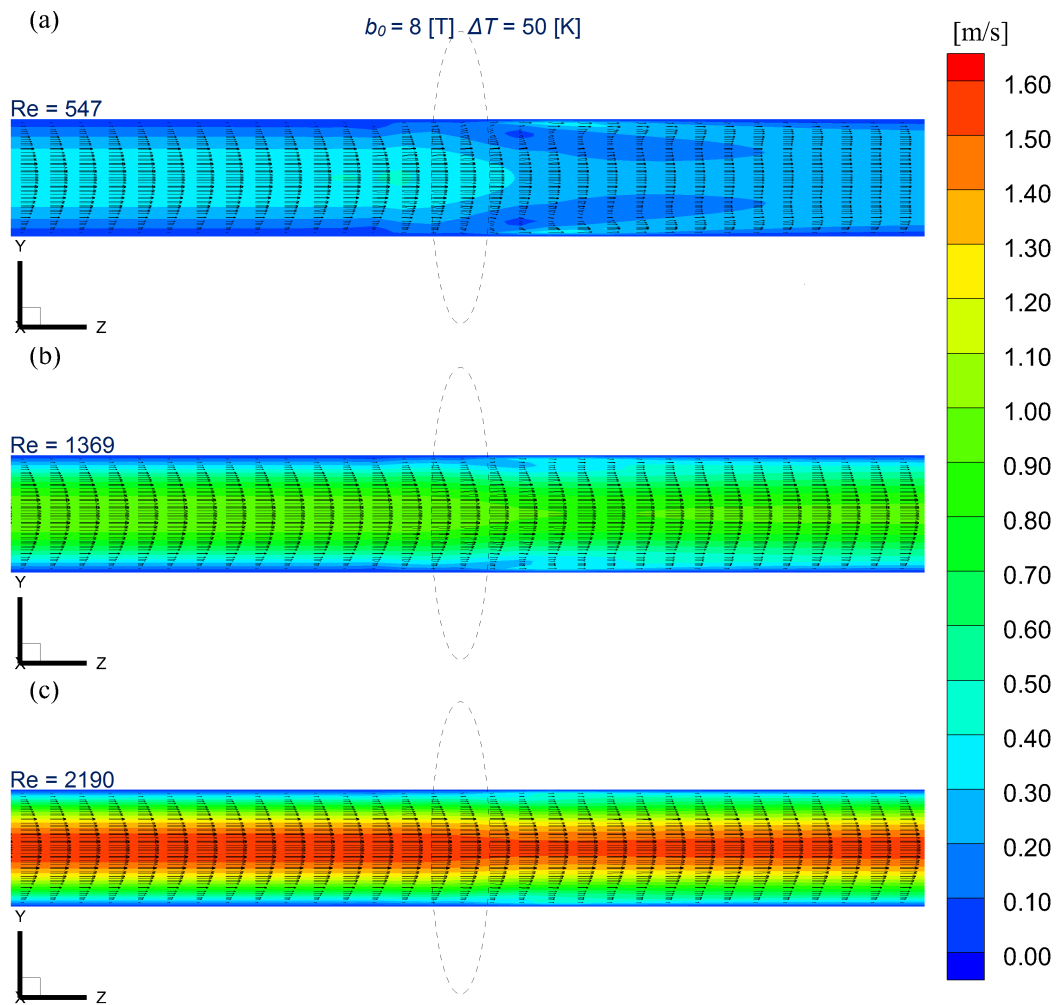


Figure 3. Velocity contours obtained in the presence of magnetic field in the pipe of $d = 0.04$ m and $l = 1$ m with average inlet velocity of: (a) 0.2 m/s, (b) 0.5 m/s, (c) 0.8 m/s.

magnetic induction in the centre of the coil $b_0 = 8$ T and constant value of the average inlet velocity $U_{avg} = 0.5$ m/s ($Re = 1369$). The varying parameter was the temperature of the wall. Figure 4 presents the influence of wall temperature variation on the velocity distributions in the magnetic field.

According to eq. (5) increase of the wall temperature led to the increase of temperature difference and indirectly to the increase of magnetic force. As in the previous case change of the magnetic force direction could be observed in the form of local acceleration of the flow near the wall. The modification of the parabolic velocity profile was connected with temperature of the wall. The flow with temperature difference of $\Delta T = 5$ [K] (figure 4(a)) behaved similarly to the flow with high average inlet velocity (figure 3(c)). In this case only the narrowing of the central area (of the highest velocity) of the flow could be reported. As the temperature increased this central area became thinner and thinner until its complete tearing (figure 4(c)).

At the same time the development of the flow's suppression proceeded, first near the wall and thereafter closer to the Z axis. The enlarging of this area was the second sign of velocity profile's deformation behind the magnetic coil.

In discussed flows, as in previously presented cases, the acceleration of the fluid near the wall

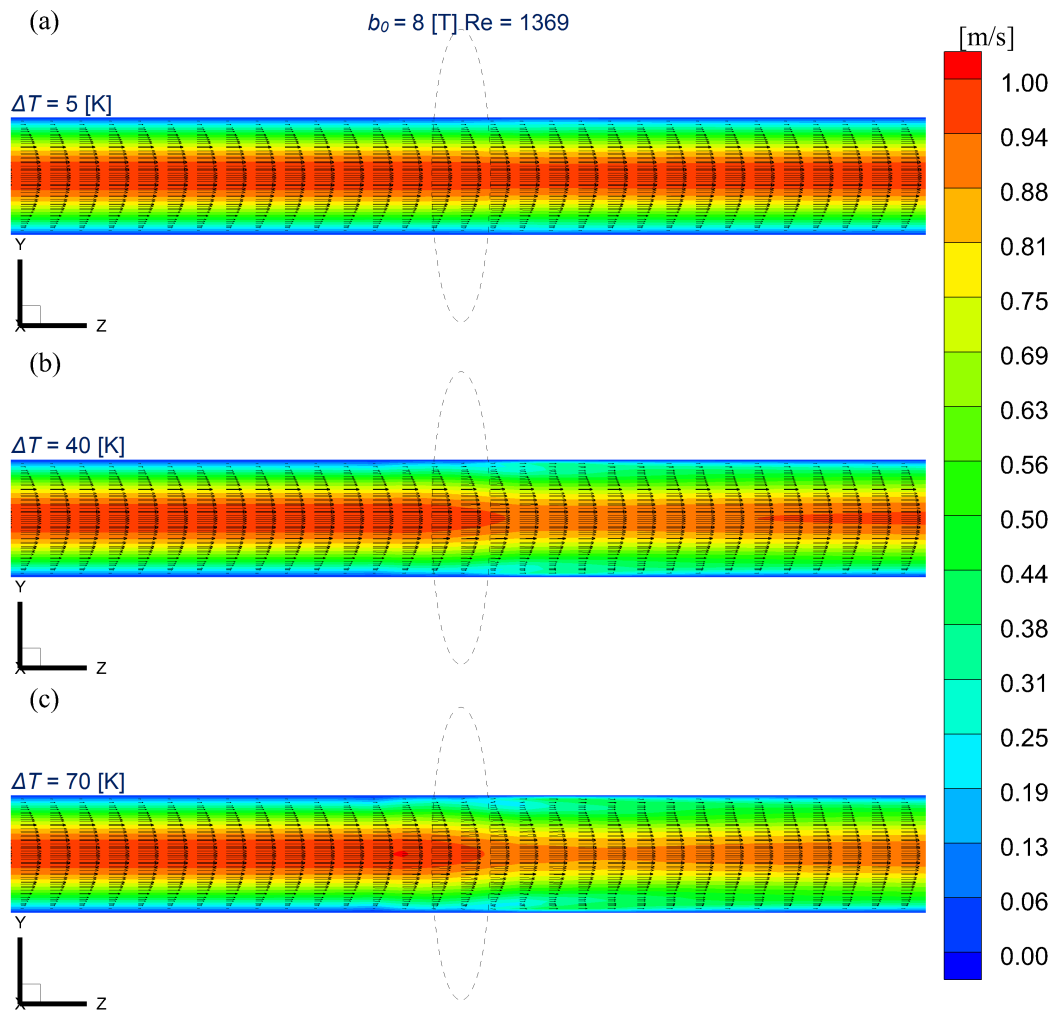


Figure 4. Velocity contours obtained in the presence of magnetic field in the pipe of $d = 0.04$ m and $l = 1$ m with temperature difference of: (a) 5 K, (b) 40 K, (c) 70 K.

caused by the magnetic force acting accordingly to flow basic direction appeared. Increase in the temperature (causing greater change in velocity profile) delayed the returning to the basic profile. Greater deformation required greater distance to return to the basic flow structure.

4.3. Analysis of magnetic induction influence on velocity and temperature distributions

The analysis of the magnetic induction in the centre of the coil influence on the velocity and temperature distributions in the pipe of diameter $d = 0.04$ m and length $l = 1$ m was conducted with constant value of the temperature difference between the flow inlet temperature and wall temperature $\Delta T = 50$ K and constant value of the average inlet velocity $U_{avg} = 0.4$ m/s ($Re = 1095$). The varying parameter was the magnetic induction in the centre of magnetic coil b_0 .

Figure 5 presents obtained velocity distributions dependent on varying parameter b_0 . As could be seen in the previous cases, also here the increase of studied parameter led to the gradual deformation of the velocity profile behind the magnetic coil in the form of narrowing of the flow central area (figure 5(b)) and its tearing (figure 5(c)). These two signs were accompanied by the deceleration zone, which at first appeared near the wall and then descended in the direction of flow axis.

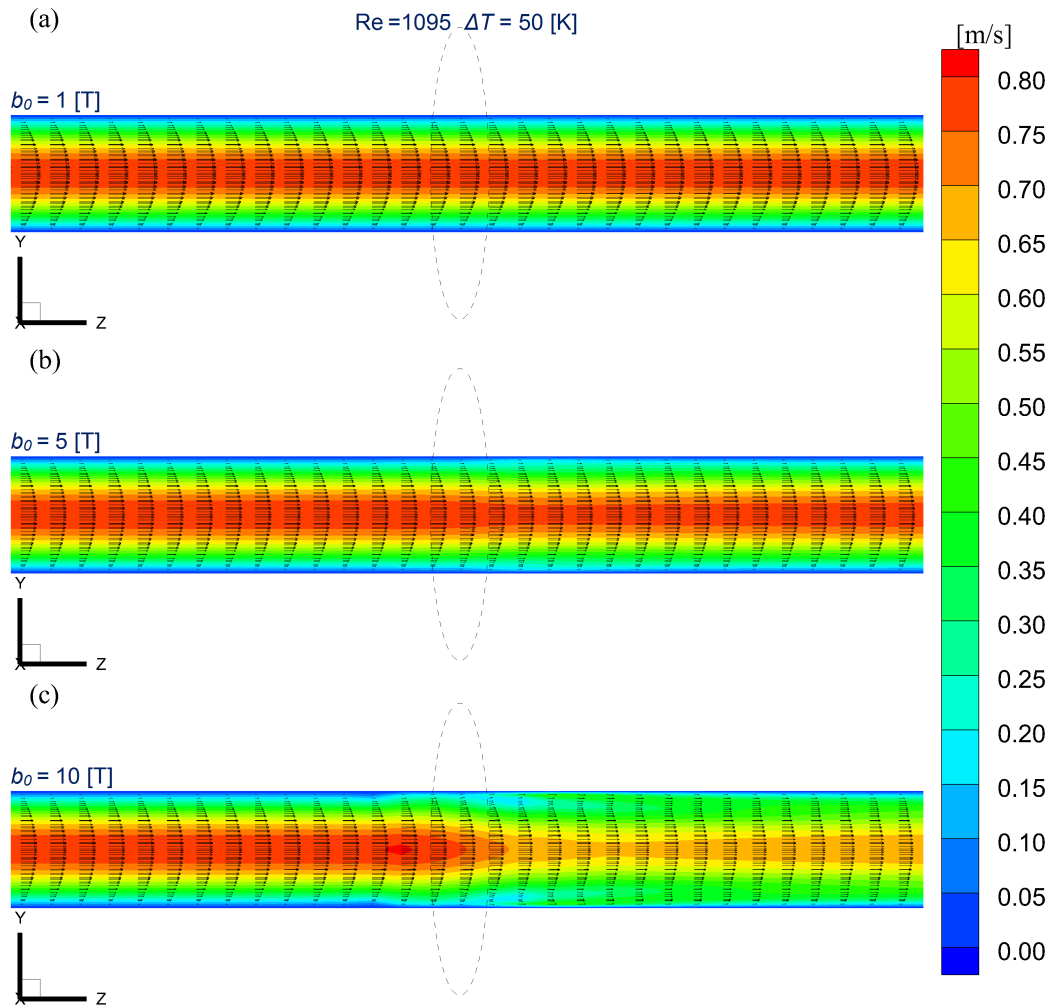


Figure 5. Velocity contours obtained in the presence of magnetic field in the pipe of $d = 0.04$ m and $l = 1$ m with the magnetic induction in the centre of the coil of: (a) 1 T, (b) 5 T, (c) 10 T.

Connection between the increasing parameter b_0 and returning distance to the basic parabolic profile remained the same as in the previous subsection.

Figure 5(a) shows that the magnetic induction of magnitude $b_0 = 1$ T didn't generate the magnetic force able to do any change of flow structure. Therefore, it could be assumed that the critical value allowing the profile change was in the range between 1 T to 5 T (and actually between 1 T to 2 T, but this data are skipped due to the lack of space available).

The similarity of results obtained with varying wall temperature and magnetic induction in the centre of the magnetic coil led to conclusion that there should be a possibility of applying the relations connecting these two effects. This conclusion is confirmed by eq.(5) where both the temperature and magnetic induction appeared.

4.4. Analysis of the flow structure in the pipe with an elbow

The analysis of the flow structure in the pipe with an elbow was conducted with constant magnitude of magnetic induction in the centre of the coil $b_0 = 10$ T, constant value of the temperature difference between the flow inlet temperature and wall temperature $\Delta T = 50$ K

and constant value of the average inlet velocity $U_{avg} = 0.023$ m/s ($Re=16$).

The distributions of velocity, temperature and magnetic force for the studied cases are presented in figures 6 and 7. Very complex three-dimensional flow structure can be observed in these figures. They show that velocity distribution as well as temperature distribution underwent strong distortions. For both variants a strong acceleration zone near the heated wall can be observed (figure 6(a) and 7(a)). It is connected with strong magnetic force influence in this area (figures 6(d) and 7(d)). The velocity in this area is about six times higher than the average inlet velocity. Aside from the acceleration zone, the deceleration zone can be also observed in the elbow. The ratio of the area between these two zones depended on heated wall variant. For variant 1 acceleration zone is much smaller than the deceleration zone. For variant 2 otherwise. Furthermore, for variant 2 the beginning of returning of the velocity profile to parabolic one can be seen.

The elbow is precluded by the ending fragment of inlet section, where for both variants vortex structures appeared. The direction of the vortex was dependant on applied variant. For variant 1 it was counter-clockwise and for variant 2 it was clockwise. The deflection of the inlet parabolic velocity profile occurred already on the section ahead of the above mentioned vortex structures. Therefore, the range of magnetic force influence is greater than in the cases described in previous subsections.

The specific temperature distribution (figures 6(c) and 7(c)) is caused by the general suppression of the flow near the magnetic coil, which is especially related to the appearance of the vortex structures. The direction of magnetic force acting can be changed after crossing the certain temperature. This temperature, called reference temperature or T_0 is an arithmetic mean of inlet fluid temperature and the heated wall temperature. The serious distortion of temperature distribution led to the explicit location of isotherm $T_0 = 5$ K. The presence of this temperature led to the appearance of reduced magnetic force zone, what can be observed in figures 6(c) and

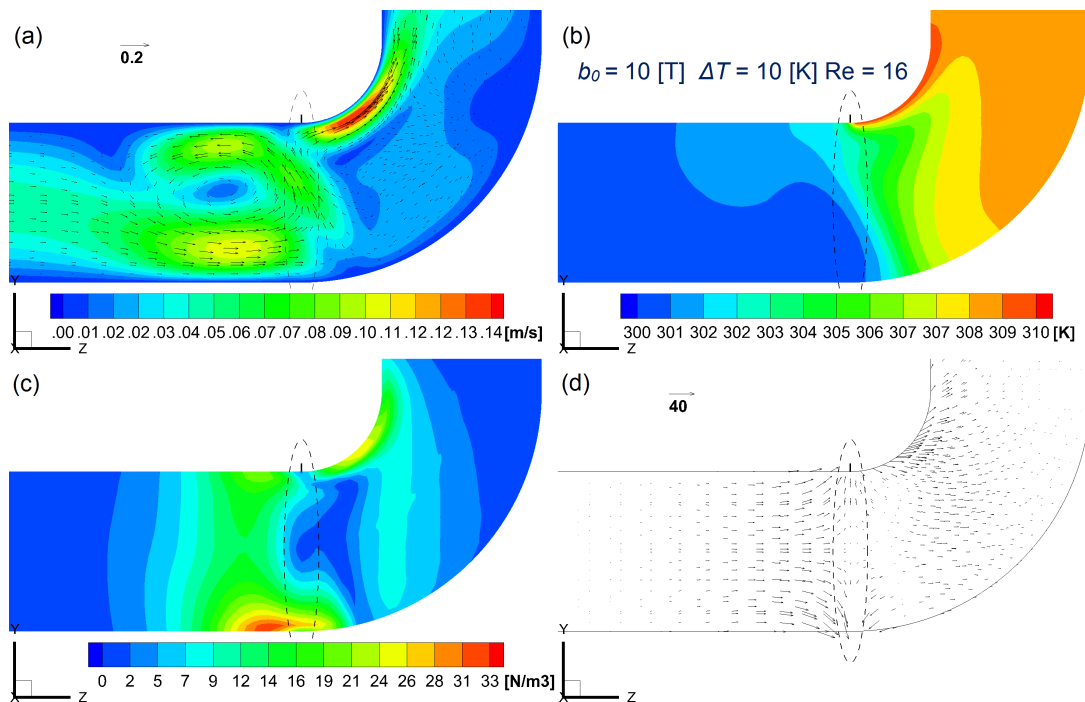


Figure 6. Flow characteristics for variant 1: (a) velocity contours and vectors, (b) temperature contours, (c) magnetic force contours, (d) magnetic force vectors.

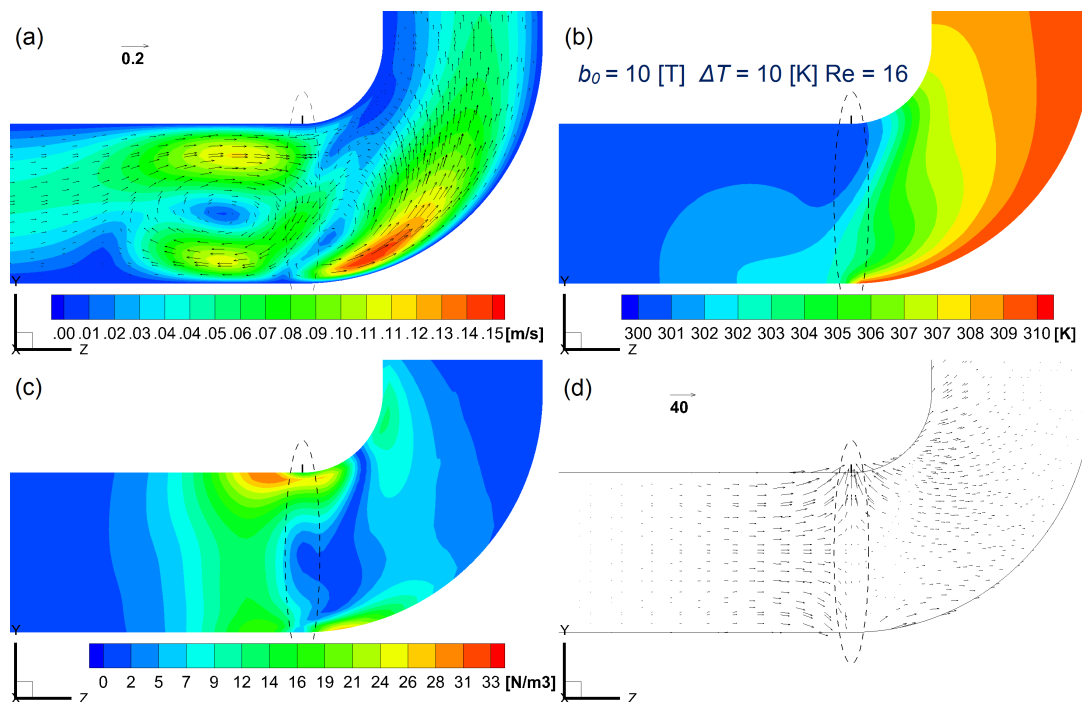


Figure 7. Flow characteristics for variant 2: (a) velocity contours and vectors, (b) temperature contours, (c) magnetic force contours, (d) magnetic force vectors.

7(c). This effect is compatible with the eq.(5).

5. Summary

A topic of paramagnetic fluid (air) forced convection under the influence of magnetic field was undertaken. It is an extension of problem analyzed by Ozoe in [18], whose results were very interesting, therefore it was decided to study the problem in details. In this paper the three-dimensional analysis of the air flow in two pipes of various diameter and with various boundary conditions under the influence of magnetic field were presented together with the straight pipe and elbow. The magnetic force acting on the paramagnetic fluid caused appearance of the acceleration, deceleration and recirculation zones and caused changes in the velocity profile. The complex three-dimensional flow structure could be obtained. It was shown that increasing inlet velocity reduced influence of the magnetic field in opposite to the increasing wall temperature or increasing magnetic induction, which magnified it. It was mentioned that all the parameters, which were varied can be combined in one, which can quantitatively described their influence on the forced convection. This topic will be continued in the next studies. Summarizing the all presented data it can be said that the magnetic field had an influence on the forced convection. However it is rather limited to the slow flows or high temperature differences and high values of magnetic induction, but it should not be neglected. There are a lot of applications for example: chemical industry, biology, medicine, porous media flow, for which the presented data are very promising.

References

- [1] Feynman R P 1967 *The Feynman Lectures on Physics* (Addison-Wesley Publishing Company)
- [2] Simon M D and Geim A I 2000 *J. App. Phys.* **87** 6200–6204
- [3] Hirota N, Ikezoe Y, Uetake H, Kaihatsu T, Takayama T and Kitazawa K 2002 *RIKEN REVIEW* **44** 159–161

- [4] Ikezoe Y, Hirota N, Nakagawa N, T and Kitazawa K 1998 *Nature* **393** 749–750
- [5] Wakayama M and Wakayama N I 2000 *Jpn. J. App. Phys.* **39** 262–264
- [6] Uetake H, Nakagawa J, Hirota N and Kitazawa K 1999 *J. App. Phys.* **86** 2924–2925
- [7] Wakayama N I 1991 *Chem. Phys. Lett.* **185** 449–451
- [8] Qi J, Wakayama N I and Yabe A 2001 *Int. J. Heat Mass Transf.* **44** 3043–3052
- [9] Tagawa T, Ujihara A and Ozoe H 2003 *Int. J. Heat Mass Transf.* **46** 4097–4104
- [10] Fornalik E, Filar P, Tagawa T, Ozoe H and Szmyd J S 2006 *Int. J. Heat Mass Transf.* **49** 2642–2651
- [11] Fornalik E, Filar P, Tagawa T, Ozoe H and Szmyd J S 2005 *Exp. Therm. Fluid Sci.* **29** 971–980
- [12] Fornalik E, Filar P, Ozoe H and Szmyd J S 2006 *Chem. Process Eng.* **27** 633–642
- [13] Bednarz T, Fornalik E, Tagawa T, Ozoe H and Szmyd J S 2005 *Int. J. Therm. Sci.* **44** 933–943
- [14] Bednarz T, Tagawa T, Kaneda M, Ozoe H and Szmyd J S 2004 *Numer. Heat Tr. A-Appl.* **46** 99–113
- [15] Wrobel W, Fornalik-Wajs E and Szmyd J S 2010 *Int. J. Heat Fluid Flow* **31** 1019–1031
- [16] Pyrda L, Kenjeres S, Fornalik-Wajs E and Szmyd J S 2012 *J. Phys.: Conf. Ser.* **395** 1–8
- [17] Kenjeres S, Pyrda L, Wrobel W, Fornalik-Wajs E and Szmyd J S 2012 *Phys. Rev. E.* **85** 1–8
- [18] Ozoe H 2005 *Magnetic Convection* (Imperial College Press)
- [19] Graetz L 1883 *Annalen der Physik und Chemie* **18** 79
- [20] Dindore V Y 2003 *Gas purification using membrane gas absorption processes* Ph.D. thesis University of Twente
- [21] Fadel A A 2009 *A novel method for the solution of convection-diffusion problems with applications to nitric oxide production and transport in vitro* Ph.D. thesis Drexel University
- [22] Fehrenbach J, Gournay F D, Pierre C and Plouraboue F 2012 *SIAM J., App. Math* **72** 99–123
- [23] Jackson J D 1998 *Classical Electrodynamics* (John Wiley and Sons Inc.)
- [24] Bednarz T 2004 *Numerical and experimental analyses of convection of paramagnetic fluid in a cubic enclosure* Ph.D. thesis Kyushu University

Acknowledgments

The present work was supported by Polish National Science Centre Project No. 2012/07/B/ST8/03109 and Academic Computer Centre CYFRONET AGH, under award no. MNiSW/IBM-BC-HS21/AGH/060/2013.